Microbeam X-ray Diffraction and Enzymatic Degradation of Poly[(*R*)-3-hydroxybutyrate] Fibers with Two Kinds of Molecular Conformations

Tadahisa Iwata,*,† Yoshihiro Aoyagi,†,§ Toshihisa Tanaka,† Masahiro Fujita,† Akihisa Takeuchi,‡ Yoshio Suzuki,‡ and Kentaro Uesugi‡

Polymer Chemistry Laboratory, RIKEN Institute, 2-1 Hirosawa, Wako-shi, Saitama 351-0198, Japan, and Japan Synchrotron Radiation Research Institute, 1-1-1 Kouto, Sayo-cho, Sayo-gun, Hyogo 678-5198, Japan

Received April 24, 2006; Revised Manuscript Received June 20, 2006

ABSTRACT: A new core−sheath structure constructed by two kinds of molecular conformations—2/1 helix (α-form) and planar zigzag (*β*-form) conformations—in biodegradable poly[(*R*)-3-hydroxybutyrate] (P(3HB)) fiber was revealed by 0.5 *μ*m microbeam X-ray diffraction in synchrotron radiation. P(3HB) fiber processed by a method combining cold-drawing and two-step-drawing has both α-form and *β*-form molecular chains in the core region, while the sheath region consists of only α-form chains. The crystallinity and orientation of α-form crystals in the core region were higher than those in the sheath region. Microbeam X-ray diffraction during two-step-drawing of cold-drawn fiber at room temperature revealed the generation mechanism of this interesting core−sheath structure at the highly ordered structural level. The *β*-form in core region was generated from amorphous chains between α-form lamellar crystals by the strong stretching of two-step-drawing. However, in the sheath region, since the α-form lamellar crystals rotated along the two-step-drawing direction, molecular chains between lamellar crystals could not elongate sufficiently. The enzymatic degradation of P(3HB) fibers was performed with an extracellular poly(hydroxybutyrate) depolymerase purified from *Ralstonia pickettii* T1. The intensity of a reflection derived from the *β*-form decreased faster than that of the α-form in X-ray fiber diagram, despite the *β*-form existing in the core region. The enzymatic degradation progressed from (1) the amorphous chains between α-form lamellar crystals in the sheath region, (2) the *β*-form molecular chains in the core region, and (3) the α-form lamellar crystals in the whole fiber. The result that the rate of enzymatic erosion of the *β*-form was faster than that of the α-form indicates that the rate of enzymatic degradation can be controlled by the molecular conformation, despite the same chemical structure.

Introduction

Poly[(*R*)-3-hydroxybutyrate] (P(3HB)), accumulated in various bacteria, is extensively studied as a biodegradable and biocompatible thermoplastic with a melting point at 180 °C.[1−3] However, it is well-known that the mechanical properties of P(3HB) materials markedly deteriorate by a process of secondary crystallization, since the glass transition temperature is ca. 4 °C.[4−6] Accordingly, P(3HB) is considered as a polymer that is difficult to use in industrial applications because of its stiffness and brittleness.

Some research groups have attempted to improve the mechanical properties of P(3HB) films[7−12] and fibers.[13−17] In the case of fibers, three groups have succeeded in obtaining melt-spun fibers with a tensile strength of 190−420 MPa from P(3HB) produced by wild-type bacteria.[13−16] However, the tensile strength of fibers is not sufficient for industrial and medical applications such as fishing line and suture. Recently, we have succeeded in producing strong and flexible fibers with a tensile strength of 1.3 GPa and elongation to break of 35% from ultrahigh-molecular-weight P(3HB) (UHMW−P(3HB)) produced by recombinant *Escherichia coli*.[17] The strong fibers were processed from amorphous fibers quenched in ice water near the grass transition temperature by a method combining cold-drawing in ice water and two-step-drawing (a second-drawing) procedure at room temperature.

The strong UHMW−P(3HB) fibers have two types of molecular conformations of P(3HB) chains: the left-handed 2/1 helix conformation (α-form) and the planar zigzag conformation (*β*-form).[17] The crystal structure of P(3HB) is well-known as an orthorhombic crystal system with unit cell parameters of $a = 0.576$ nm, $b = 1.320$ nm, and c(fiber axis) $= 0.596$ nm and the 2/1 helix molecular conformation (α-form).[18,19] The *β*-form was first observed in stretched P(3HB) film by Yokouchi et al.[18] and further confirmed in a slow cold-drawing film of poly[(*R*)-3-hydroxybutyrate-*co*-(*R*)-3-hydroxyvalerate] (PHB/V)) by Orts et al.[20] The *β*-form is introduced from the orientation of free molecular chains in amorphous regions between α-form lamellar crystals in stretched films.[18,20] Recently, this *β*-form was further observed in two-step drawn films applied to hot- or cold-drawn films by Aoyagi et al.[11] and Iwata et al.,[12] and the mechanism for generating the *β*-form during two-step-drawing was investigated by time-resolved wide- and small-angle X-ray scattering of synchrotron radiation together with the measurement of stress−strain curves.[21]

The microbeam X-ray diffraction of synchrotron radiation is a powerful technique to reveal the distribution of different molecular structures and crystal orientation in a monofilament, the twisting of lamellar crystals in spherulites, the in situ transition of the crystal structures, etc. In fact, microbeam diffraction has been utilized to understand the fine structures of viscose rayon fibers,[22] spider silk,[23] spherulites of P(3HB),[24]

* To whom all correspondence should be addressed: Tel +81-48-467-9586; Fax +81-48-462-4667; e-mail tiwata@riken.jp.
† RIKEN Institute.
‡ Japan Synchrotron Radiation Research Institute.
§ Present address: Akebono R&D center, Ltd., 5-4-71 Higashi, Hanyu-shi, Saitama 348-8511, Japan.

10.1021/ma060908v CCC: $33.50
Published on Web 07/19/2006

P(3HB) copolymers,[25] and the poly(latic acid)/atactic-P(3HB) blend.[26] In our previous communication, we demonstrated a microbeam X-ray diffraction of UHMW−P(3HB) monofilament and revealed that the UHMW−P(3HB) fiber has a core−sheath structure with two kinds of molecular conformations: a 2/1 helix conformation (α-form) in the sheath region and a planar zigzag conformation (β-form) in the core region.[17] However, the mechanism for generating this interesting core−sheath structure is unclear at this point.

Until now, the enzymatic degradations of P(3HB) have been mainly studied using melt-crystallized films with various degrees of crystallinity[27−29] and uniaxially oriented films.[10] The extracellular poly(hydroxybutyrate) (PHB) depolymerases isolated from various environments degrade P(3HB) materials first at the amorphous region and subsequently at the crystal region. Furthermore, it was revealed that the rate of enzymatic degradation can be controlled by the degree of crystallnity.[10,30] On the other hand, the mechanism for degrading lamellar crystals has been extensively investigated using solution-grown single crystals. The adsorption of extracellular PHB depolymerase on P(3HB) single crystals was examined using the immuno-gold labeling technique, which demonstrated a homogeneous distribution of enzymes on the surface of crystals.[31,32] However, the enzymatic degradation of P(3HB) single crystals progresses from the edges of crystals and along their long axis as making a small crystal fragment, not from the crystal surface despite homogeneous adsorptions of enzyme molecules on the crystal surface.[31−37] These results indicate that an enzyme molecule cannot degrade an ester unit in the chain-folding part of the molecular chain on the crystal surface by the steric hindrance and that the rate of enzymatic degradation depends on the amount of lateral side of crystals. However, until now, there is no information for the mechanism of enzymatic degradation at the molecular conformation level of polymer chains.

In this paper, we report first the detail analysis of core−sheath structure in the P(3HB) monofilament consisting of two kinds of different molecular conformations by using microbeam X-ray diffraction focused to 0.5 μm with the Fresnel zone plate optics. Furthermore, a new generation mechanism of core−sheath structure is proposed on the basis of the microbeam X-ray diffraction of the necking part of the monofilament. A novel enzymatic degradation behavior of monofilament with two kinds of molecular conformations is further presented by using an extracellular PHB depolymerase purified from *Ralstonia pickettii* T1.

Experimental Section

P(3HB) Fibers. The *Escherichia coli* strain XL1-Blue harboring a stable plasmid pSYL105 containing *Ralstonia eutropha* H16 PHA biosynthesis genes[38] was used to produce ultrahigh-molecular-weight P(3HB) (UHMW−P(3HB), according to the method reported previously.[9,10,39] The weight-average molecular weight and polydispersity of UHMW−P(3HB) used in this study were 5.3×10^6 and 1.7, respectively.

Melt spinning of UHMW−P(3HB) was carried out using a laboratory-size screw extruder equipped with a single nozzle with an inner diameter of 1 mm. UHMW−P(3HB) was extruded at 200 °C, which was 20 °C higher than the melting point of the sample. The extruder was taken up at 28 m/min and directly into an ice water bath placed 15 cm below the nozzle to obtain the amorphous fiber. The amorphous fibers were stretched by cold-drawing up to 600% of their initial length in ice water by using two sets of rollers. The two-step-drawing (a second-drawing step) was applied against the oriented amorphous fibers by a stretching machine at room temperature and then annealed in an autoclave at 50 °C with weak tension to increase the crystallinity.

Microbeam X-ray Diffraction. The microbeam wide-angle X-ray diffraction was carried out at the BL47XU beamline with a wavelength of 0.15497 nm at 8 keV of synchrotron radiation at SPring-8, Harima, Japan. The experimental focus beam size was obtained as 0.5 μm by using the Fresnel zone plate optics.[40] A P(3HB) monofilament with 40 μm diameter was linearly scanned perpendicular to the fiber axis with a step width of 2 μm between the individual frames. In the case of two-step-drawing (a second-drawing step), a cold-drawn P(3HB) fiber was fixed on the handmade stretching machine and stretched to 600% of initial length. After stretching, scanning was performed perpendicular to the stretching direction with a step of 10 μm and parallel to the stretching direction with a step of 30 μm between the individual frames. The diffraction patterns were recorded with a Be-windowed, 4-in.-diameter X-ray image intensifier (V7739P, Hamamatsu Photonics, Japan) coupled with a CCD camera (C4880-10-14A, Hamamatsu Photonics, Japan) with exposure times of 5 s. The camera length was 110 mm. Diffraction data were processed with the program R-axis Display Software (Rigaku, Japan). Crystal orientation was evaluated from the width of the azimuthal direction of the equatorial (020) reflection. The rotation angle of lamellar crystals was estimated as the angle between the equatorial line in the X-ray fiber diagram and the perpendicular line to the fiber axis.

Enzymatic Degradation of Fibers. The extracellular poly(hydroxybutyrate) (PHB) depolymerase from *Ralstonia pickettii* T1 was purified to electrophoretic homogeneity according to the method of Tanio et al.[41] The enzymatic degradation of the P(3HB) fibers was carried out at 37 °C in 0.1 M potassium phosphate buffer (pH 7.4) with shaking at 120 rpm. Sample fibers were placed in small glass bottles containing 1 mL of phosphate buffer. The reaction was started by the addition of 5 μL of an aqueous solution of PHB depolymerase (200 μg/mL). Sample fibers were washed with distilled water and dried to constant weight in vacuo, and X-ray diffraction and scanning electron microscope observation were performed.

Wide-Angle X-ray Diffraction. The wide-angle X-ray diffraction patterns of P(3HB) fibers before and after partial enzymatic degradation were recorded on a Rigaku RINT UltraX 18 type X-ray generator operated at 40 kV and 110 mA. The scan was carried out in the $\theta/2\theta$ reflection mode in the 2θ range of 6−60° and a scan speed of 2°/min.

Scanning Electron Microscopy. Scanning electron micrographs were taken by using a JEOL JSM-6330F microscope, operated at an acceleration voltage of 5 kV, after samples were coated with gold using a SANYU DENSHI SC-701 quick coater.

Optical Microscopy. The morphologies during two-step-drawing of P(3HB) cold-drawn fibers were observed with an optical microscope (Nikon OPTI-PHOTO-2) equipped with crossed polarizers, a CCD camera (Ikegami IF-8500), and an image analyzer (OLYMPUS XL-10).

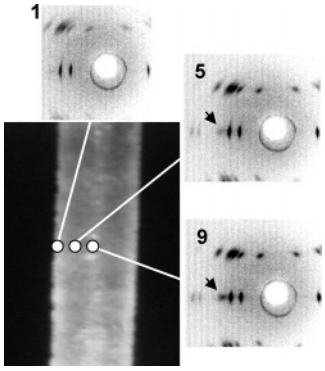

Figure 1. Microbeam X-ray fiber diagrams of cold-drawn and two-step-drawn P(3HB) monofilament recorded from the selected three marked points in the microscope image (left picture). No. 1, 5, and 9 indicate the diffraction position of edge, middle between edge and center, and center of monofilament, respectively. The arrows indicate a reflection assigned as β-form.

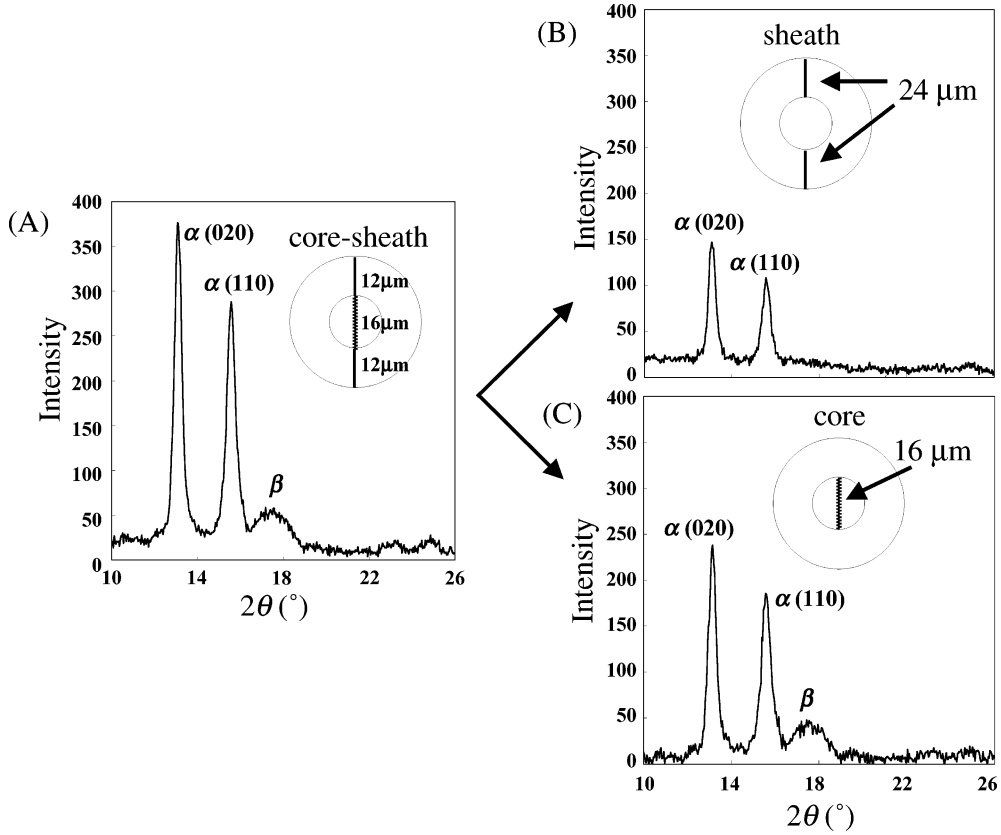

Figure 2. (A) Intensity profile of equatorial line in X-ray fiber diagram of no. 9 in Figure 1. The α(020) and α(110) reflections were indexed by the α-form crystal parameters, and β indicates the equatorial reflection of β-form crystal. Intensity profile of no. 9 (A) was divided to the sheath region (B, sheath region is 24 μm) and the core region (C, core region is 16 μm).

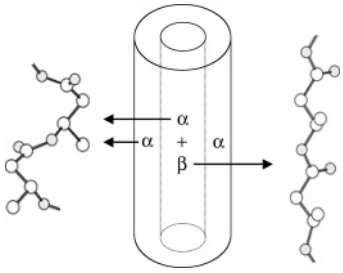

Figure 3. Schematic display of the core−sheath structure of P(3HB) monofilament with two kinds of molecular conformations: 2/1 helix conformation (α-form) and planar zigzag conformation (β-form).

Results and Discussion

Core−Sheath Structure of P(3HB) Fiber. UHMW−P(3HB) fibers with tensile strength of 1.3 GPa, elongation to break of 35%, and Young's modulus of 18.1 GPa were produced by a method combining cold-drawing in ice water and two-step-drawing (a second-drawing step) at room temperature. The microbeam X-ray diffraction was performed with synchrotron radiation at SPring-8, Japan, with a beam size focused to 0.5 μm by Fresnel zone plate optics. Figure 1 shows the P(3HB) monofilament image with a diameter of 40 μm and the selected microbeam X-ray fiber diagrams recorded from the marked points in the optical microscopic image. In the microbeam X-ray fiber diagram of no. 1 (edge part), all the reflections were indexed by only α-form crystal parameters with a 2/1 helix conformation. However, in no. 5 (middle point between edge and center) and no. 9 (center part) diagrams, one can see a new reflection in the equatorial line, indexed by the β-form (planar zigzag conformation) together with α-form crystals.

The intensity profile of the microbeam X-ray diffraction pattern of no. 9 where is a center position of fiber (Figure 2A) was divided into two profiles: the fields of the sheath region and core region. The core pattern has been derived by subtract-

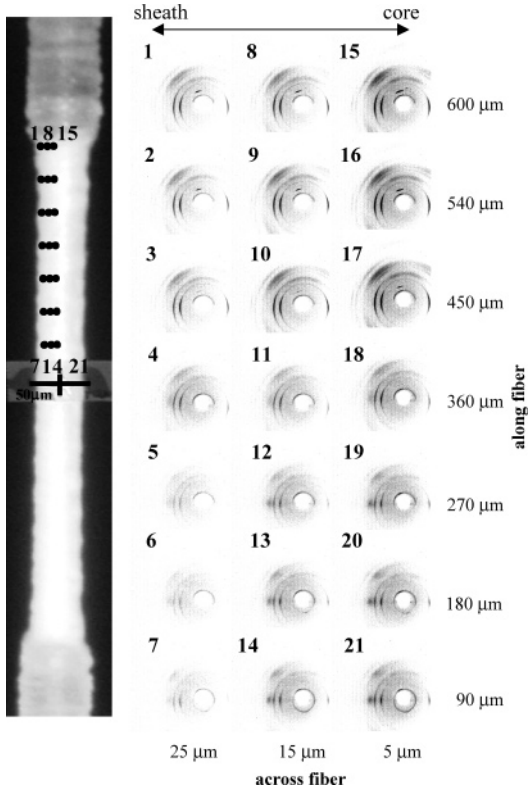

Figure 4. Microbeam X-ray fiber diagrams of P(3HB) monofilament during two-step-drawing at room temperature, recorded from the marked points in the microscope image. The step width of breadth and length is 10 μm and 90 μm, respectively.

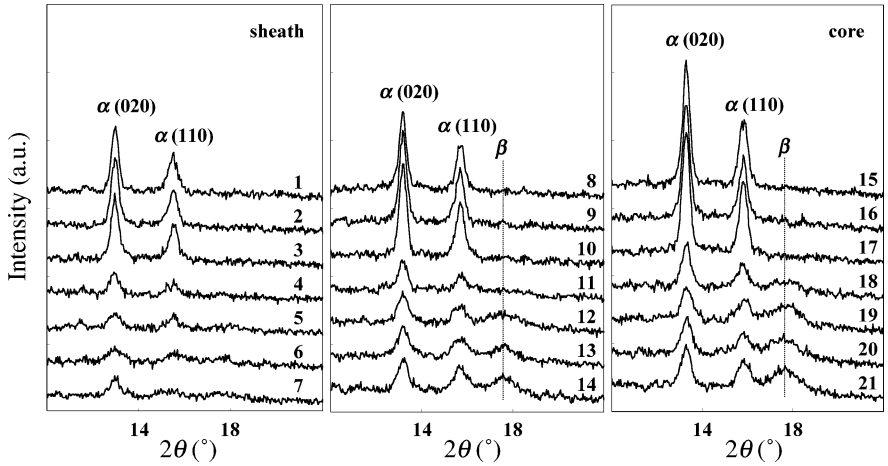

Figure 5. Intensity profiles of equatorial lines in X-ray fiber diagrams as shown in Figure 4.

ing the sheath pattern from the pattern recorded at the center of the fiber (no. 9). Parts B and C of Figure 2 show an intensity profile of the sheath region (24 μm) and the core region (16 μm), respectively. While the sheath region consists of only α-form crystal, both α- and β-forms exist in the core region. When the intensities of α(020) and α(110) reflections between sheath and core regions were compared, the intensities in the core region (Figure 2C) were higher than those in the sheath region (Figure 2B), although the volume of the sheath region is larger than that of the core region. It is well-known that the rate of crystallization in the sheath region is faster than that of the core region, since the cooling rate in the sheath region is faster that that of the core region. Accordingly, the crystallinity in the core region is higher than that in the sheath region, and our experimental result is in agreement with previous knowledge.

On the other hand, while the sheath region consists of only α-form crystals, the core region has two types of crystals with both α-form and β-form. This result clearly indicates that this P(3HB) monofilament has a core−sheath structure with two kinds of molecular conformations: 2/1 helix (α-form) and planar zigzag (β-form) conformations of P(3HB) chains. Until now, many kinds of core−sheath fibers are processed by using two kinds of different polymers. Furthermore, the viscose-rayon fiber with the orientation distribution of crystal blocks was revealed by an electron diffraction method.[22] However, as far as we know, this type of core−sheath structure that consists of two kinds of molecular conformations in one polymer has not been reported previously. Figure 3 shows a schematic display of the P(3HB) monofilament with a new core−sheath structure having two kinds of molecular conformations of α-form and β-form.

Generation Mechanism of a New Core−Sheath Structure. To reveal the generation mechanism of a new core−sheath structure of P(3HB) fiber, microbeam X-ray diffraction experiments were performed during two-step-drawing of a cold-drawn P(3HB) fiber at room temperature. A cold-drawn fiber was set on a handmade stretching machine and stretched to 600% of initial length. Necking drawing was observed in optical microscopic image as shown in Figure 4. Microbeam X-ray diffractions were attempted to all the marked points in image with a step of 10 μm perpendicular to and 90 μm along the two-step-drawing direction. Figure 5 shows the line profile data obtained from equatorial lines in microbeam X-ray fiber diagrams in Figure 4. At the edge region (no. 1−7), it is difficult to find a β-form reflection close to the 2θ angle of 17.5° (d-spacing is 0.460 nm). However, in the core region, one can see observe a β-form reflection, especially in no. 12−14 and 18−21. The intensities of α(020) and α(110) in no. 18−21 decreased compared with those in no. 15−17, suggesting that a part of lamellar crystals seems to be broken by a two-step-drawing. However, the intensity of the β-form in no. 18−21 increased proportionally depending on the drawing ratio, despite the intensities of α(110) and α(020) remaining unchanged. This result indicates that the β-form generates from the amorphous region between α-form lamellar crystals by two-step-drawing.

Figure 6A shows the crystal rotation angle (θ) of α-form lamellar crystals calculated by the angle between the equatorial line in the X-ray fiber diagram and the line perpendicular to the fiber axis. The 0° of θ value indicates that lamellar crystal aligns perpendicular to the fiber axis, and molecular chains align parallel to the drawing direction. The θ values in the core region (no. 15−21, across fiber = 5 μm) and in the sheath region (no. 1−7, across fiber = 25 μm) are 0° to 8° and −4° to −14°, respectively, suggesting that lamellar crystals in the sheath region rotate more largely than in the core region. Thus, the stretching force during two-step-drawing directly penetrates to amorphous chains in the core region, and molecular chains seem to be elongated parallel to the drawing direction. Accordingly, the intensity of β-form reflection in the core region (no. 18−21) is higher than that in other regions (no. 11−14). On the other hand, it is difficult to observe a β-form reflection in X-ray fiber diagrams in the sheath region (no. 1−7). In a sheath region, the elongation of molecular chains between lamellar crystals is avoided by the rotation of lamellar crystals. The (020) orientation of α-form lamellar crystals as shown in Figure 6B further supports our hypothesis. The orientation in the core region (no. 15−21) is higher than that in the sheath region (no. 1−7) as a whole. The highest value in the core region is 0.921 but 0.903 in the sheath region.

We monitored a necking behavior during two-step-drawing of cold-drawn P(3HB) fiber by using an optical microscope equipped with crossed polarizers. Figure 7A shows an optical microscopic image during two-step-drawing of P(3HB) cold-drawn fiber. The brilliant parts indicate the crystal blocks of lamellar crystal. It was observed that the crystal blocks clearly rotate along the drawing direction in the sheath region, and finally all the crystals align parallel to the drawing.

On the basis of the results of microbeam X-ray diffraction and optical microscopic observation during two-step-drawing of cold-drawn P(3HB) fiber, a new mechanism of an interesting core−sheath fiber is drawn in Figure 7B. It is concluded that the planar zigzag conformation (β-form) generates from the amorphous molecular chains between lamellar crystals in the core region of fiber. In the sheath region, molecular chains are

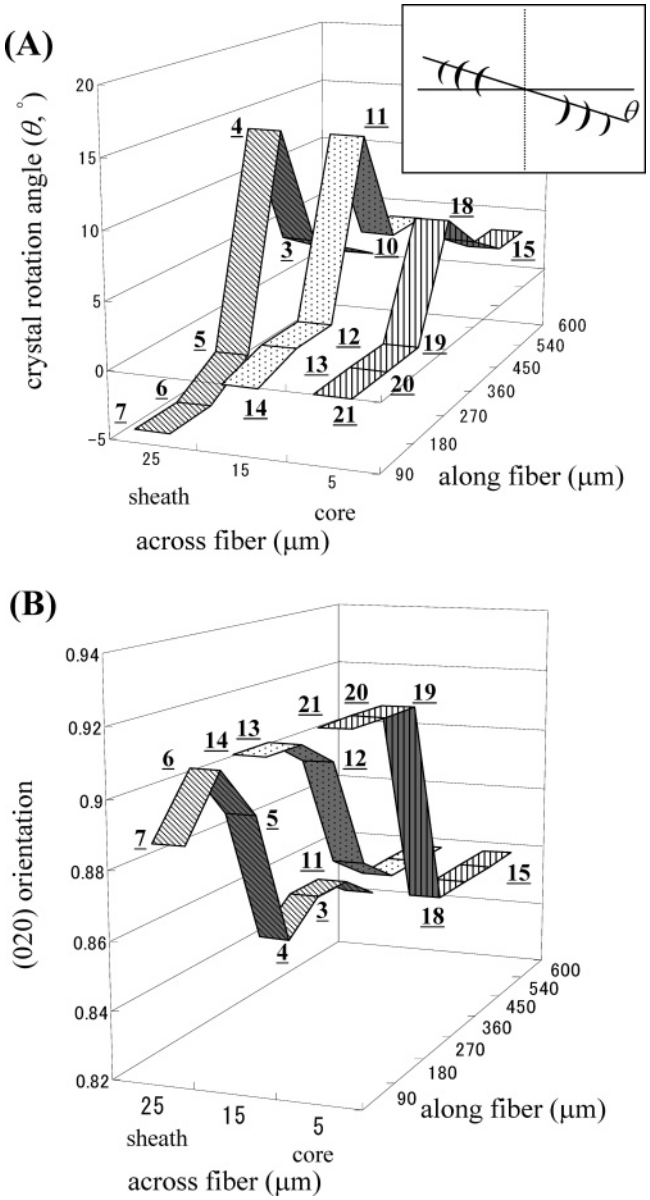

Figure 6. (A) Crystal rotation angle (θ) and (B) (020) orientation of α-form lamellar crystals, calculated from X-ray fiber diagrams in Figure 4. Crystal rotation angle (θ) is defined as the angle between the equatorial line in X-ray fiber diagram and the line perpendicular to drawing direction. The 0° of θ indicates that lamellar crystals align perpendicular to the drawing direction. The (020) orientation was obtained from azimuthal scans of the (020) reflection in X-ray fiber diagrams. Each number with an underline indicates a file number of X-ray fiber diagram in Figure 4.

not strongly elongated by the rotation of lamellar crystals during two-step-drawing. As a result, two-step-drawn P(3HB) fiber has an interesting core−sheath structure with two kinds of molecular conformations.

Enzymatic Degradation of P(3HB) Fibers with Core−Sheath Structure. Enzymatic degradation of P(3HB) fibers with core−sheath structure consisting of two kinds of molecular conformations, 2/1 helix (α-form) and planar zigzag (β-form), was performed in an aqueous solution containing extracellular PHB depolymerase from *Ralstonia pickettii* T1 at 37 °C. Figure 8 shows the scanning electron micrographs of a P(3HB) fiber before and after partial enzymatic degradation. It was revealed that this strong fiber was degraded by PHB depolymerase, and the enzymatic erosion progressed from the fiber surface.

Figures 9 and 10 show X-ray fiber diagrams and X-ray diffraction patterns of P(3HB) fibers before and after partial

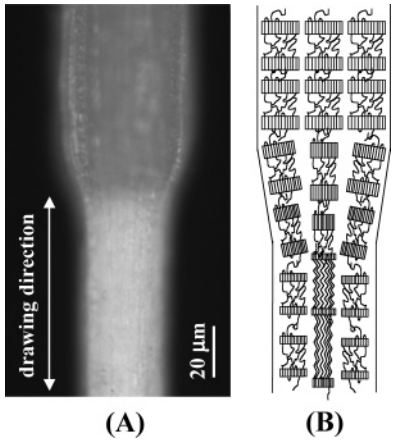

Figure 7. (A) Optical microscope image during two-step-drawing of cold-drawn amorphous fiber at room temperature. The brilliant parts indicate the crystal blocks of lamellar crystal. The arrows indicate the two-step-drawing directions. (B) Schematic display of two-step-drawing behavior. The α-form lamellar crystals and β-form planar zigzag conformation chains exist in the core region.

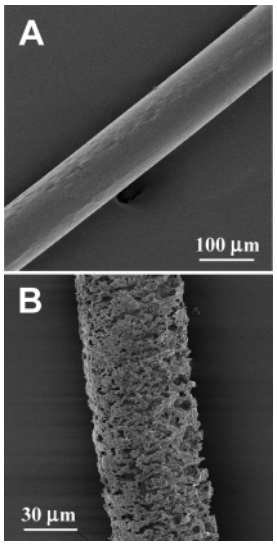

Figure 8. Scanning electron micrographs of P(3HB) fiber before (A) and after (B) partial enzymatic degradation in an aqueous solution of PHB depolymerase purified from *Ralstonia pickettii* T1 at 37 °C.

enzymatic degradation, respectively. While the intensities of α-form crystals remained unchanged before and after enzymatic degradation, the intensity of β-form decreased, despite β-form existing in core region. This result indicates that the planar zigzag conformation (β-form) is degraded faster than the 2/1 helix conformation (α-form). Thus, the rate of enzymatic erosion can be controlled by the molecular conformation, despite the same chemical structure.

In our previous report, we presented a similar phenomenon in the enzymatic degradation of poly(β-propiolactone) which having two kinds of molecular structures and three kinds of crystal structures.[42] Furuhashi et al. reported that β-form with planar zigzag conformation in cold-drawn and annealed film degraded faster than α-form with 2/1 helix conformation in hot-drawn and annealed film. On the basis of these results, it is suggested that the molecular conformation and crystal structure are important and common factors for controlling the rate of enzymatic degradation in polyesters.

In the case of P(3HB) monofilament with core−sheath structure, β-form degraded faster than α-form, although β-form existed in the core region in the fiber. The degradation

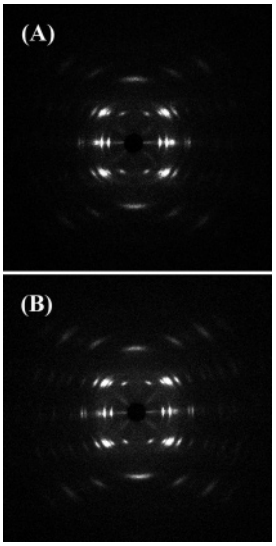

Figure 9. X-ray fiber diagrams of P(3HB) fibers before (A) and after (B) partial enzymatic degradation in an aqueous solution of PHB depolymerase purified from *Ralstonia pickettii* T1 at 37 °C.

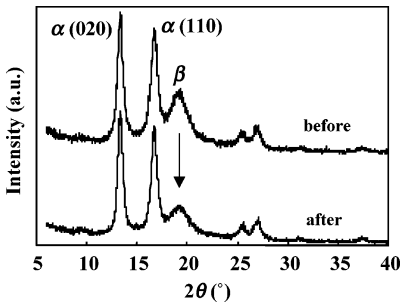

Figure 10. Intensity profiles of equatorial lines in X-ray fiber diagrams before and after partial enzymatic degradation in an aqueous solution of PHB depolymerase purified from *Ralstonia pickettii* T1 at 37 °C. The α and *β* indicate the reflections derived from α-form and *β*-form crystal, respectively.

mechanism is presented in Figure 11. Figure 11A shows the schematic display of highly ordered structure of P(3HB) fiber with two kinds of molecular conformations. The sheath region consists of two domains that are lamellar crystals with 2/1 helix conformation (α-form) and amorphous region between these lamellar crystals. On the other hand, in the core region, *β*-form domains exist between lamellar crystals by high orientation of amorphous chains. It is well-known that the enzymatic degradation progresses from the amorphous region in material surface. Accordingly, the enzymatic degradation of P(3HB) fibers was first progressed from the amorphous region between α-form lamellar crystals in the fiber surface (sheath region), as shown in Figure 11B. Furthermore, the enzyme molecules can penetrate the inside of fiber by degrading the amorphous regions. Then, molecular chains of *β*-form seem to be easily attacked by enzyme molecules, rather than those of α-form, because the steric hindrance against the ester bond in planar zigzag conformation is less than in helix conformation. As a result, the intensity induced from *β*-form decreased and α-form crystal remained unchanged after partial enzymatic degradation. In a longer enzymatic degradation test, it is confirmed that whole fibers are completely degraded by PHB depolymerase.

More recently, we succeeded to reveal the crystal structure of PHB depolymerase from *Penicillium funiculosum*.[43] The trimer substrate of (*R*)-3-hydroxybutyrate with planar zigzag conformation was perfectly bound in crevice for active site. This result supports that *β*-form (planar zigzag conformation) is degraded faster than α-form (2/1 helix conformation), which was obtained from the enzymatic degradation of P(3HB) fibers with two kinds of molecular conformations. These results indicate that the rate of enzymatic degradation can be controlled by the molecular conformations of polymers.

Conclusion

A new core−sheath structure of P(3HB) fiber, prepared by a method of combining cold-drawing in ice water and a second-drawing step at room temperature, was revealed by microbeam X-ray diffraction using synchrotron radiation. P(3HB) fiber has an interesting core−sheath structure with two kinds of molecular conformations; α-form (2/1 helix conformation) and *β*-form (planar zigzag conformation). The core region consists of both α- and *β*-forms, while the sheath region consists of only α-form. The generation mechanism of a new core−sheath structure was investigated by microbeam X-ray diffraction and optical microscopic observation during two-step-drawing of cold-drawn fiber. The *β*-form is generated from amorphous chains between lamellar crystals by the direct penetration of stretching force in core region. However, it was found that in the sheath region molecular chains are not strongly elongated by the rotation of lamellar crystals. The enzymatic degradation of P(3HB) fiber with core−sheath structure was investigated by using an extracellular PHB depolymerase from *Ralstonia pickettii* T1. The enzymatic degradation of *β*-form was faster than that of α-form, suggesting that molecular conformation is one of the important factors for determining the rate of enzymatic degradation, despite the same chemical structure.

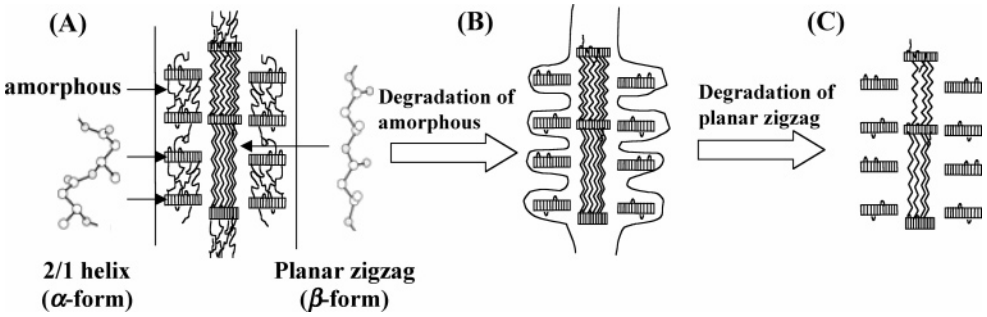

Figure 11. Schematic display of enzymatic degradation behavior of P(3HB) fibers with two kinds of molecular conformations: α-form (2/1 helix conformation) and *β*-form (planar zigzag conformation). (A) Before enzymatic degradation: P(3HB) fiber has a core−sheath structure with two kinds of molecular conformations. Amorphous region exists between lamellar crystals of α-form in the sheath region, and *β*-form exists between lamellar crystals of α-form in the core region. (B) After partial enzymatic degradation: the amorphous region between lamellar crystals (α-form) is degraded preferentially. (C) When further enzymatic degradation makes progress, *β*-form chains in core region are degraded. Accordingly, the intensity of *β*-form decreased, despite the α-form remaining unchanged.

Acknowledgment. This work has been supported by a Grant-in-Aid for Young Scientists (A) from the Ministry of Education, Culture, Sports, Science and Technology (MEXT) of Japan (No. 15685009) and by a grant from Ecomolecular Science Research provided to the RIKEN Institute. The synchrotron radiation experiments were performed at the SPring-8 with the approval of the Japan Synchrotron Radiation Research Institute (JASRI) (Proposals 2003B0054-NL2b-np, 2004B0016-ND1b-np, and 2005A0307-ND1b-np).

References and Notes

(1) Alper, R.; Lundgren, D. G.; Marchessault, R. H.; Cote, W. A. *Biopolymers* **1963**, *1*, 545.
(2) Doi, Y. *Microbial Polyesters*; VHC Publishers: New York, 1990.
(3) Anderson, A. J.; Dawes, E. A. *Microbiol. Rev.* **1990**, *54*, 450.
(4) Holmes, P. A. In Bassett, D. C., Ed.; *Developments in Crystalline Polymers*; Elsevier Applied Science: London, 1988; Vol. 2, pp 1−65.
(5) De Koning, G. J. M.; Lemstra, P. J. *Polymer* **1993**, *34*, 4089.
(6) Scandola, M.; Ceccorulli, G.; Pizzoli, M. *Macromol. Chem., Rapid Commun.* **1989**, *10*, 47.
(7) De Koning, G. J. M.; Scheeren, A. H. C.; Lemstra, P. J.; Peeters, M.; Reynaers, H. *Polymer* **1994**, *35*, 4598.
(8) Barham, P. J.; Keller, A. *J. Polym. Sci., Polym. Phys. Ed.* **1986**, *24*, 69.
(9) Kusaka, S.; Iwata, T.; Doi, Y. *J. Macromol. Sci., Pure Appl. Chem.* **1998**, *35*, 319.
(10) Kusaka, S.; Iwata, T.; Doi, Y. *Int. J. Biol. Macromol.* **1999**, *25*, 87.
(11) Aoyagi, Y.; Doi, Y.; Iwata, T. *Polym. Degrad. Stab.* **2003**, *79*, 209.
(12) Iwata, T.; Tsunoda, K.; Aoyagi, Y.; Kusaka, S.; Yonezawa, N.; Doi, Y. *Polym. Degrad.* Stab. **2003**, *79*, 217.
(13) Gordeyev, S. A.; Nekrasov, Y. P. *J. Mater. Sci., Lett.* **1999**, *18*, 1691.
(14) Schmack, G.; Jehnichen, D.; Vogel, R.; Tändler, B. *J. Polym. Sci., Part B: Polym. Phys.* **2000**, *38*, 2841.
(15) Yamane, H.; Terao, K.; Hiki, S.; Kimura, Y. *Polymer* **2001**, *42*, 3241.
(16) Furuhashi, Y.; Imamura, Y.; Jikihara, Y.; Yamane, H. *Polymer* **2004**, *45*, 5703.
(17) Iwata, T.; Aoyagi, Y.; Fujita, M.; Yamane, H.; Doi, Y.; Suzuki, Y.; Takeuchi, A.; Uesugi, K. *Macromol. Rapid Commun.* **2004**, *25*, 1100.
(18) Yokouchi, M.; Chatani, Y.; Tadokoro, H.; Teranishi, K.; Tani, H. *Polymer* **1973**, *14*, 267−272.
(19) Okamura, K.; Marchessault, R. H. In Ramachandra, G. N., Ed.; *Conformation of Biopolymers*; Academic Press: New York, 1967; Vol. 2, pp 709−720.
(20) Orts, W. J.; Marchessault, R. H.; Bluhm, T. L.; Hamer, G. K. *Macromolecules* **1990**, *23*, 5368.
(21) Iwata, T.; Fujita, M.; Aoyagi, Y.; Doi, Y.; Fujisawa, T. *Biomacromolecules* **2005**, *6*, 1803.
(22) Müller, M.; Riekel, C.; Vuong, R.; Chanzy, H. *Polymer* **2000**, *41*, 2627.
(23) Riekel, C.; Madsen, B.; Knight, D.; Vollrath, F. *Biomacromolecules* **2000**, *1*, 622.
(24) Gazzano, M.; Focarete, M. L.; Riekel, C.; Scandola, M. *Biomacromolecules* **2000**, *1*, 604.
(25) Tanaka, T.; Fujita, M.; Takeuchi, A.; Suzuki, Y.; Uesugi, K.; Doi, Y.; Iwata, T. *Polymer* **2005**, *46*, 5673.
(26) Gazzano, M.; Focarete, M. L.; Riekel, C.; Scandola, M. *Biomacromolecules* **2004**, *5*, 553.
(27) Barham, P. J.; Keller, A.; Otun, E. L.; Holmes, P. A. *J. Mater. Sci.* **1984**, *19*, 2781.
(28) Kumagai, Y.; Kanesawa, Y.; Doi, Y. *Makromol. Chem.* **1992**, *193*, 53.
(29) Tomasi, G.; Scandola, M.; Briese, B. H.; Jendrossek, D. *Macromolecules* **1996**, *29*, 507.
(30) Iwata, T. *Macromol. Biosci.* **2005**, *5*, 689.
(31) Iwata, T.; Doi, Y.; Kasuya, K.; Inoue, Y. *Macromolecules* **1997**, *30*, 833.
(32) Iwata, T.; Doi, Y.; Tanaka, T.; Akehata, T.; Shiromo, M.; Teramachi, S. *Macromolecules* **1997**, *30*, 5290.
(33) Hocking, P. J.; Revol, J.-F.; Marchessault, R. H. *Macromolecules* **1996**, *29*, 2467.
(34) Hocking, P. J.; Marchessault, R. H.; Timmins, M. R.; Lenz, R. W.; Fuller, R. C. *Macromolecules* **1996**, *29*, 2472.
(35) Nobes, G. A. R.; Marchessault, R. H.; Chanzy, H.; Briese, B.; Jendrossek, D. *Macromolecules* **1996**, *29*, 8330.
(36) Iwata, T.; Shiromo, M.; Doi, Y. *Macromol. Chem. Phys.* **2002**, *203*, 1309.
(37) Marchessault, R. H.; Kawada, J. *Macromolecules* **2004**, *37*, 7418.
(38) Lee, S. Y.; Lee, K. M.; Chang, H. N.; Steinbüchel, A. *Biotechnol. Bioeng.* **1994**, *44*, 1337.
(39) Kusaka, S.; Abe, H.; Lee, S. Y.; Doi, Y. *Appl. Microbiol. Biotechnol.* **1997**, *47*, 140.
(40) Suzuki, Y.; Takeuchi, A.; Takano, H.; Ohigashi, T.; Takenaka, H. *Jpn. J. Appl. Phys.* **2001**, *40*, 1508.
(41) Tanio, T.; Fukui, T.; Shirakura, Y.; Saito, T.; Tomita, K.; Kaiho, T.; Masamune, S. *Eur. J. Biochem.* **1982**, *124*, 71.
(42) Furuhashi, Y.; Iwata, T.; Kimura, Y.; Doi, Y. *Macromol. Biosci.* **2003**, *3*, 462.
(43) Hisano, T. Kasuya, K.; Tezuka, Y.; Ishii, N.; Kobayashi, T.; Shiraki, M.; Oroudjev, E.; Hansma, H.; Iwata, T.; Doi, Y.; Saito, T.; Miki, K. *J. Mol. Biol.* **2006**, *356*, 993.

MA060908V